EFFECTS OF AIR-FILLED CAVITY DISTRIBUTION ON ACOUSTIC ABSORPTION PERFORMANCE OF ANECHOIC COATINGS

Van Hai Trinh[1]

Abstract: *Submarines are often covered with resonant sound absorbers known as anechoic coatings or tiles in order to avoid detection by sonar. A simulation-based model is developed for predicting the acoustic properties of underwater anechoic structures having matrix viscoelastic materials containing air-filled cavities. In order to validate the proposed modeling, the preliminary numerical results of an anechoic configuration are first compared with available literature data. Then, a systematic investigation of the effects of the periodic air-filled cavity distribution on the acoustic absorbing property of anechoic layer is conducted. It can be stated from the obtained results that tuning the air-filled cavity distribution such as the location and porosity allows broadening and tailoring the acoustic performance of considered anechoic coating over some specific bands or a whole range of frequency.*

Keywords: Air-filled cavity, local structure, absorption property, anechoic coating.

1. INTRODUCTION

The complicated multicomponent and multiscale structures are often designed for submarines requiring high-quality acoustic stealth coatings. By considering their microstructure, these anechoic structures can be categorized: air-filled cavity, multi-layer composite, and pressure-resisting (Qian and Li 2017). A submarine with its multi-layered cover under detection by the active sonar depicted in Figure 1. In Alberich anechoic coating layer with air-filled cavity array, two types of resonance mechanisms are known: one is due to the radial motion of the hole wall and the other to the drum-like oscillations of the cover layer (Gaunaurd 1985). Additionally, the developed structure allows broadening and tailoring its acoustic performance by tuning some geometrical parameters of the air bubble distribution. It is noted that macroscopic acoustic properties are highly dependent on the local microstructural features of each individual layer as well as the layer configuration (Yang and Sheng 2017).

Different approaches have been established in the literature for predicting the link between the microstructural parameters of anechoic structures and their macroscopic acoustic performance: analytical (Gaunaurd 1977, Leroy, Strybulevych et al. 2009, Meng 2014, Sharma, Skvortsov et al. 2017), numerical (Ma, Scott et al. 1980, Hladky‐Hennion and Decarpigny 1991, Sohrabi and Ketabdari 2018, Zhong, Zhao et al. 2019), and experimental methods (Leroy, Bretagne et al. 2009, Leroy, Strybulevych et al. 2009, Leroy, Strybulevych et al. 2015). Various analytical studies addressing structure-acoustic problems exist including typically: transfer matrix method, effective medium model. However, these analytical models often make simplifications on the displacement field and geometry, thereby imposing limitations on the type of problem to be solved. On contract, the numerical approach (e.g., the finite element method) is more flexible in dealing with complex structures which allows analyzing harmonic wave propagation in viscoelastic gratings with periodic or random distributions with single- or multi-layered structures.

Thus, a simulation-based model based on finite element scheme is developed for predicting the acoustic properties of anechoic structures having matrix viscoelastic materials containing air-filled cavities.

[1] *Faculty of vehicle and energy engineering (FVEE), Le Quy Don technical university, 236, Hoang Quoc Viet, Bac Tu Liem, Ha Noi.*

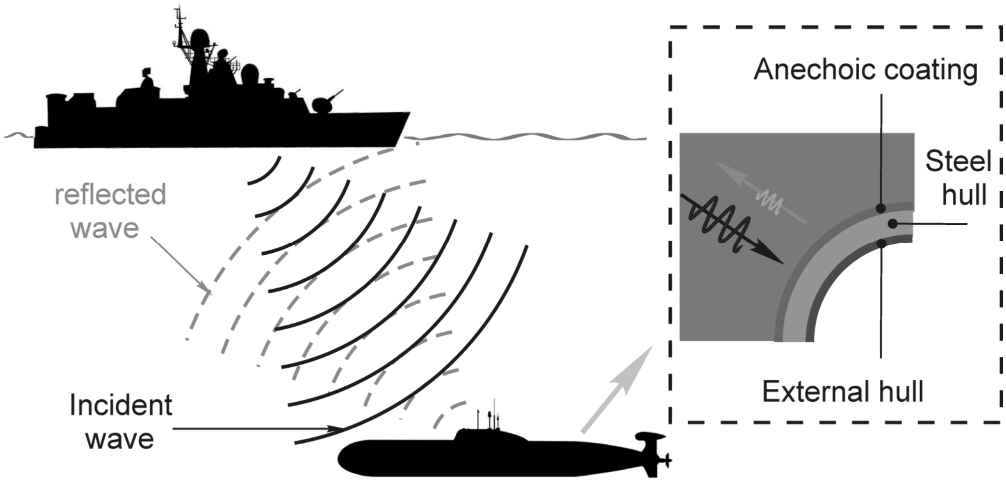

Figure 1. A submarine with its multi-layered cover under detection by the active sonar

2. NUMERICAL FRAMEWORK

In acoustics, the pressure of sound wave can be calculated as a function of time and location (Hopkins 2012). Complex form is often used for representing the sound waves (Easwaran and Munjal 1993), and the harmonic wave is depicted at frequency ω and wave number k as,

$$p_0(t,\mathbf{x}) = A_0 \exp[j(\omega t - k\mathbf{x} - \phi_0)], \quad (1)$$

where A_0 is the amplitude, ϕ_0 is the initial phase, and j is the imaginary unit.

In order to understand the acoustic behavior of sound absorbing materials, we first need to understand what occurs when sound wave travel through these media. It can be known that the sound wave interacts with the material or object surface and may be absorbed, transmitted and reflected (see Figure 2). Therefore, the incident wave energy would be partly separated into three corresponding components.

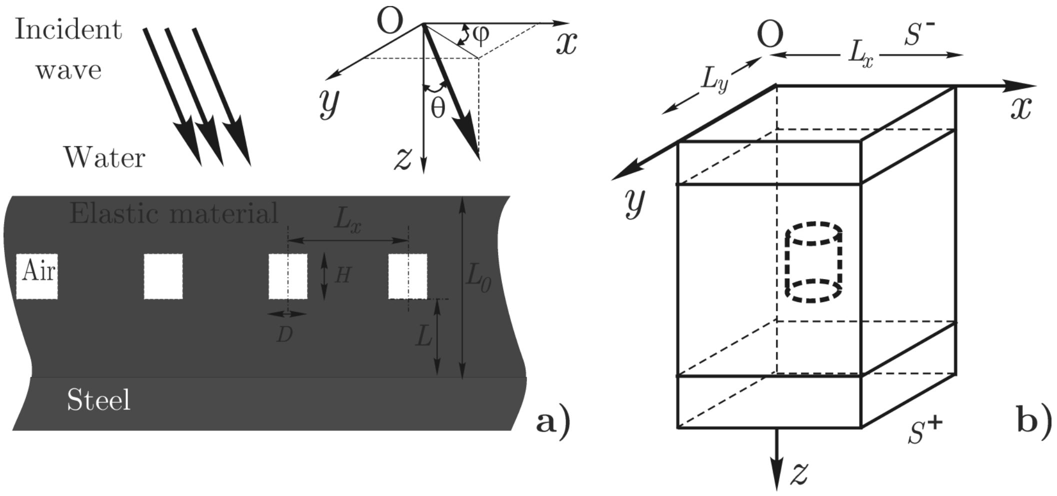

Figure 2. Absorption structure includes a viscoelastic material and a backing steel (a) and schematic description of the representative unit cell (b).

The structure is excited by a harmonic plane wave from the semi-infinite fluid medium. The expression of the incident wave is:

$$p_{\text{in}}(x,y,z) = \exp\left[-jk\left(x\sin\theta\cos\varphi + y\sin\theta\cos\varphi + z\cos\theta\right)\right], \quad (2)$$

where the time dependence exp($-j\omega t$) as shown in Eq. (1) has been omitted for clarity, θ and φ denote the direction of the incident wave (see Figure 2.a).

According to Bloch's theorem, if the structure has the periodic distance Lx in the x direction and Ly in the y direction, any space function χ (e.g., pressure, displacement..etc) satisfies the following relation (Hladky - Hennion and Decarpigny 1991):

$$\chi\left(x+L_x, y+L_y, z\right)=\chi\left(x, y, z\right)\exp\left(jL_x k\sin\theta\cos\varphi\right)\exp\left(jL_y k\sin\theta\sin\varphi\right). \quad (3)$$

Figure 2.b shows the computing model of one unit cell among the multilayer slab, where S^- and S^+ surfaces parallel to the xOy plane limit the finite element mesh from the half infinite backing and water domains for incidence, respectively. The external incident wave and the reflected wave in the domain above the S^- surface and the transmitted wave in the domain above the S^+ surface can be written in the general forms:

$$\begin{aligned} p^-\left(x,y,z\right) &= p_{\text{in}}\left(x,y,z\right)+p_r\left(x,y,z\right) \\ &= p_{\text{in}}\left(x,y,z\right)+\sum_{m,n=-\infty}^{+\infty} R_{mn}\exp\left[-j\left(k_{nmx}x+k_{ny}y-k_{mn}z\right)\right], \\ p^+\left(x,y,z\right) &= p_t\left(x,y,z\right)=\sum_{m,n=-\infty}^{+\infty} T_{mn}\exp\left[j\left(k_{mx}x+k_{ny}y+k_{mn}z\right)\right], \end{aligned} \quad (4)$$

where $k_{mx}=2m\pi/L_x+k\sin\theta\cos\varphi$, $k_{ny}=2n\pi/L_y+k\sin\theta\cos\varphi$, and $k_{mn}^2=k^2-k_{mx}^2-k_{ny}^2$. R_{mn} and T_{mn} are the reflection and transmission coefficients corresponding to the (m, n)th mode.

In the coupled structure-acoustic problem, the discretized form of the governing equation can be written as (Sandberg, Wernberg et al. 2008, Fu, Jin et al. 2015):

$$\begin{bmatrix} \boldsymbol{M}_s & 0 \\ \rho_0 c_0 \boldsymbol{H}^{\mathrm{T}} & \boldsymbol{M}_f \end{bmatrix}\begin{bmatrix} \ddot{\boldsymbol{u}}_s \\ \ddot{\boldsymbol{p}}_f \end{bmatrix}+\begin{bmatrix} \boldsymbol{K}_s & -\boldsymbol{H} \\ 0 & \boldsymbol{K}_f \end{bmatrix}\begin{bmatrix} \boldsymbol{u}_s \\ \boldsymbol{p}_f \end{bmatrix}=\begin{bmatrix} \boldsymbol{f}_s \\ \boldsymbol{f}_f \end{bmatrix}, \quad (5)$$

where $\boldsymbol{M}$, $\boldsymbol{C}$ and $\boldsymbol{K}$ are the global mass, damping, and stiffness matrices, respectively. Subscripts 's' and 'f' denote the solid and the fluid domains, respectively. $\boldsymbol{u}_s$ is the nodal displacement vector in the structural domain and $\boldsymbol{p}_f$ is the nodal pressure vector in the fluid domain, whereas $\boldsymbol{f}_s$ and $\boldsymbol{f}_f$ are the nodal structural force and the nodal acoustic pressure vectors, respectively.

By solving Eq. (5), the nodal values of the pressure on the incident surface (p^-) and transmission surface (p^+) can be obtained. Thus, the unknown coefficient R_{mn} and T_{mn} are can be deduced from two sets of equations establishing based on the number of known pressure values in the corresponding surfaces. It can be noted that each unknown coefficient requires one nodal pressure value. Thus, the anechoic performance of an acoustic sound absorbing medium is defined by absorption coefficients (α) as (Hladky - Hennion and Decarpigny 1991, Wen, Zhao et al. 2011, Fu, Jin et al. 2015):

$$\alpha=1-\left|R\right|^2-\left|T\right|^2, \text{ with } R=\sqrt{\sum_{k_{mn}^2>0}\left|R_{mn}\right|^2} \text{ and } T=\sqrt{\sum_{k_{mn}^2>0}\left|T_{mn}\right|^2} \quad (6)$$

3. RESULTS AND DISCUSSION

In the validation step, to verify our modeling, the analytical model and measurement data proposed by V. Leroy el al. in Ref. (Leroy, Strybulevych et al.

2015) are used. The acoustical model of anechoic tile is structured with a soft elastic layer having an air cavity array with L_x=L_y and backing by a steel layer. The elastic material layer has a thickness of $L_0 = 230$ μm and cylindrical cavities of diameter $D = 24$ μm and height $H = 12$ μm (see left part of Figure 2). The Young's modulus, density, and Poisson's ratio of the steel hull are respectively 2.16×10^{11} Pa, 7800 kg/m^3, and 0.3. Figure 3 presents the results corresponding the cases of L_x=50 μm (left) and L_x=120 μm (right), the obtained good agreements validate our model.

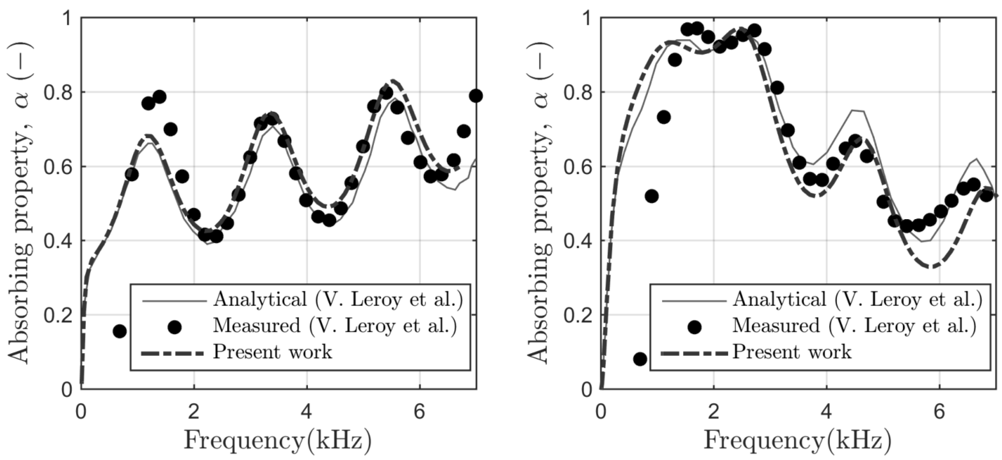

Figure 3. Comparison of sound absorptions obtained from the present work with the analytical model and experimental data proposed in Ref. (Leroy, Strybulevych et al. 2015).

Next, we present how the distribution density and location of air cavity affect to the acoustical behavior of the single air array anechoic. Figure 4 presents the absorbed energy proportions as a function of porosity $\phi = 25\pi D^2 H / (L_x^2 L_0)$ for two configurations of L = 0 (left) and $L = L_0/2$ (right). Here, the porosity ranges from 0.11 (%) to 1.02 (%) corresponding varying of the air cavity distance L_x from 50 μm to 150 μm. It can be noted from the obtained charts that: for L = 0, anechoic tiles with low porosities show high acoustic absorption capability at low frequency range, while high porosity anechoic tile provides a better property of α at high frequency band; when air cavities locating in the middle of anechoic layer ($L = L_0/2$), its poor acoustic property seems do not affect by the porosity, (see also Figure 5). In addition, anechoic coatings show high absorption performance (~75 %) in compared with the steel block alone with 88% of the reflected energy and 12 % transmitted energy fraction is (Leroy, Strybulevych et al. 2015).

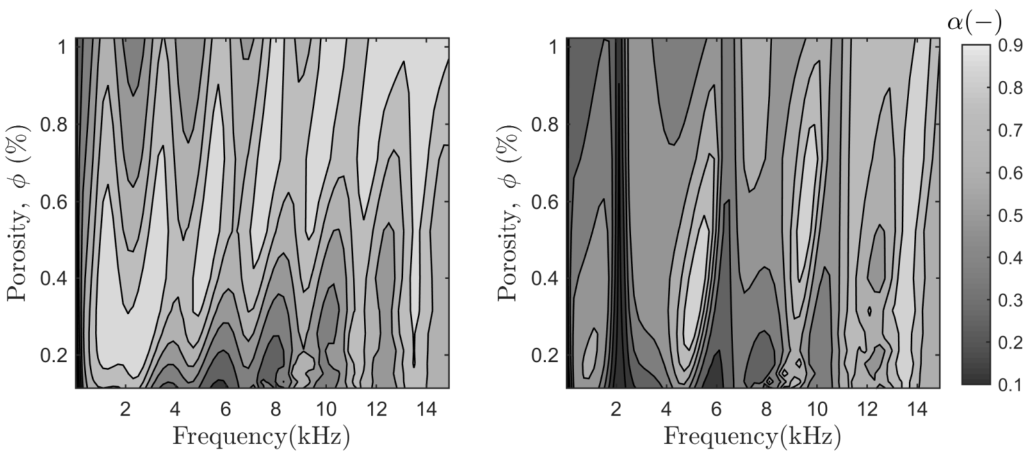

Figure 4. Porosity dependence of absorbing property of anechoic coatings.

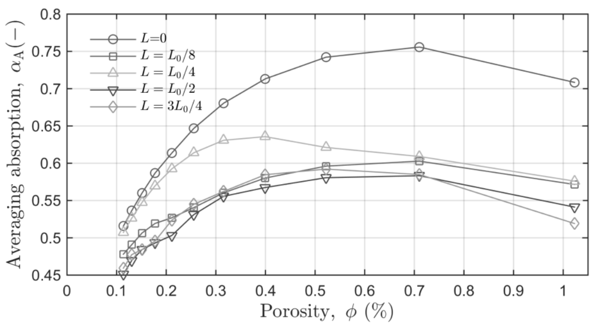

Figure 5. Effects of air cavity distribution on averaging absorption property.

In order to further investigate the effect of air-filled cavity distribution on acoustic performance, the averaging absorption property as $\alpha_A = \frac{1}{N}\sum_{i=1}^{N}\alpha_i(f_i)$ is estimated from a set of values of α_i at N the discrete angular frequencies f_i used in the frequency range of interest. As shown in Figure 5, the higher distance of air-filled cavity from the backing steel layer, the lower acoustic absorption property. In detailed, for the case without distance between air cavity and steel hull, the averaging absorbing property is higher than 70 % with porosity larger than 0.37 %.

4. CONCLUSION

A numerical approach is presented to investigate the link between microstructure and acoustic properties of an anechoic structure with periodic air cavities. Very good agreements are observed between the present numerical results with both the reference analytical model and experimental data, which validate the proposed finite element procedure. From systematically investigated results, it is seen that two tuning geometrical parameters of the air cavity affect strongly to the acoustical properties. Specially, the porosity has a strong effect on the level of absorbed energy. This interesting point shows a good opportunity to achieve the desired absorption properties in an entire frequency range by tuning together two parameters mentioned here and also others fixed such as thickness layer L_0 and ratios D/H and H/L_0.

REFERENCES

Easwaran, V. and M. Munjal (1993). *"Analysis of reflection characteristics of a normal incidence plane wave on resonant sound absorbers: A finite element approach."* The Journal of the Acoustical Society of America 93(3): 1308-1318.

Fu, X., Z. Jin, Y. Yin and B. Liu (2015). *"Sound absorption of a rib-stiffened plate covered by anechoic coatings."* The Journal of the Acoustical Society of America 137(3): 1551-1556.

Gaunaurd, G. (1977). *"One‐dimensional model for acoustic absorption in a viscoelastic medium containing short cylindrical cavities."* The Journal of the Acoustical Society of America 62(2): 298-307.

Gaunaurd, G. (1985). *"Comments on 'Absorption mechanisms for waterborne sound in Alberich anechoic layers'."* Ultrasonics 23(2): 90-91.

Hladky‐Hennion, A. C. and J. N. Decarpigny (1991). *"Analysis of the scattering of a plane acoustic wave by a doubly periodic structure using the finite element method: Application to Alberich anechoic coatings."* The Journal of the Acoustical Society of America **90**(6): 3356-3367.

Hopkins, C. (2012). *Sound insulation*, Routledge.

Leroy, V., A. Bretagne, M. Fink, H. Willaime, P. Tabeling and A. Tourin (2009). "*Design and characterization of bubble phononic crystals*." Applied Physics Letters **95**(17): 171904.

Leroy, V., A. Strybulevych, M. Lanoy, F. Lemoult, A. Tourin and J. H. Page (2015). "*Superabsorption of acoustic waves with bubble metascreens*." Physical Review B **91**(2): 020301.

Leroy, V., A. Strybulevych, M. Scanlon and J. Page (2009). "*Transmission of ultrasound through a single layer of bubbles*." The European Physical Journal E **29**(1): 123-130.

Ma, T.-C., R. Scott and W. H. Yang (1980). "*Harmonic wave propagation in an infinite elastic medium with a periodic array of cylindrical pores*." Journal of Sound and Vibration **71**(4): 473-482.

Meng, T. (2014). "*Simplified model for predicting acoustic performance of an underwater sound absorption coating.*" Journal of Vibration and Control **20**(3): 339-354.

Qian, C. and Y. Li (2017). "*Review on Multi-scale Structural Design of Submarine Stealth Composite.*" DEStech Transactions on Engineering and Technology Research(icaenm).

Sandberg, G., P.-A. Wernberg and P. Davidsson (2008). *Fundamentals of fluid-structure interaction.* Computational aspects of structural acoustics and vibration, Springer**:** 23-101.

Sharma, G. S., A. Skvortsov, I. MacGillivray and N. Kessissoglou (2017). "*Acoustic performance of gratings of cylindrical voids in a soft elastic medium with a steel backing.*" The Journal of the Acoustical Society of America **141**(6): 4694-4704.

Sohrabi, S. H. and M. J. Ketabdari (2018). "*Numerical simulation of a viscoelastic sound absorbent coating with a doubly periodic array of cavities*." Cogent Engineering **5**(1): 1-21.

Wen, J., H. Zhao, L. Lv, B. Yuan, G. Wang and X. Wen (2011). "*Effects of locally resonant modes on underwater sound absorption in viscoelastic materials.*" The Journal of the Acoustical Society of America **130**(3): 1201-1208.

Yang, M. and P. Sheng (2017). "*Sound absorption structures: From porous media to acoustic metamaterials.*" Annual Review of Materials Research **47**: 83-114.

Zhong, J., H. Zhao, H. Yang, J. Yin and J. Wen (2019). "*On the accuracy and optimization application of an axisymmetric simplified model for underwater sound absorption of anechoic coatings.*" Applied Acoustics **145**: 104-111.

Tóm tắt:

ẢNH HƯỞNG CỦA PHÂN BỐ KHOANG KHÍ ĐẾN HIỆU QUẢ HẤP THỤ ÂM CỦA LỚP VỎ TIÊU ÂM

Tàu ngầm thường được bọc bằng lớp hấp thụ âm cộng hưởng hay được gọi là lớp phủ hoặc ngói không phản xạ để tránh phát hiện bởi các thiết bị định vị thủy âm (sonar). Một mô hình dựa trên mô phỏng số được phát triển để dự đoán tính chất âm học của các cấu trúc không phản xạ dưới nước làm bằng vật liệu đàn-nhớt và chứa các khoang khí bên trong. Để kiểm chứng mô hình đề xuất, các kết quả số sơ bộ của một cấu hình lớp không phản xạ trước tiên được so sánh với dữ liệu đã được công bố. Sau đó, bài báo tiến hành khảo sát có hệ thống ảnh hưởng của sự phân bố có trật tự các khoang khí lên tính chất hấp thụ âm của lớp không phản xạ. Có thể nói từ các kết quả thu được rằng việc điều chỉnh phân bố khoang khí như vị trí và độ xốp cho phép mở rộng và điều chỉnh hiệu suất âm thanh của lớp phủ không phản xạ trên một số dải cụ thể hoặc toàn bộ dải tần.

Từ khóa: Khoang khí, tham số hình học cơ sở, đặc tính hấp thụ, ngói tiêu âm.

Ngày nhận bài: 29/8/2019

Ngày chấp nhận đăng: 10/9/2019